

# Characterizing iron reducing microorganisms from anoxic ferruginous lake sediments

Glass Laboratory  
School of Earth and Atmospheric Sciences

Bianca Costa  
Fall 2018

Faculty Advisors

Dr. Jennifer Glass

Dr. Spyros Pavlostathis

## **Abstract**

Lake Matano, Indonesia is a well-known ancient ocean analogue as its anoxic ecosystem in the subsurface sediments allow the growth of microorganisms capable of mediating anaerobic oxidation coupled to iron reduction. An anoxic, ferric iron rich BSR was kept for 163 days to culture iron reducing bacteria in an environmental sample from Lake Matano sediment. Microscopy analysis was performed periodically to look for morphology trends using DAPI staining. Phylogenetic analysis was performed using CARD-FISH microscopy to target the *Geobacter* genus, known for electroactive abilities through *pilA* and interactions with iron particles. Cell counts correlated with iron reduction throughout the culturing period indicating iron reducing microorganisms were present in the environmental sample. Filamentous, coccus, bacillus and vibrio morphologies were observed through the culturing period with vibrio and bacillus being predominant at later stages of the culture. Particle association instances were observed at days 20, 62, 86 and 126 and DIET interactions at day 86. Characterizing these microorganisms opens a broad range of possibilities for wastewater treatment (strip mining groundwater contamination), use in bioelectrochemical systems biofilms (due to external electron transport *pilA*) and understanding the importance of this microorganisms in Iron cycling.

## **Abbreviations**

SBR	Sequencing Batch Bioreactor
CARD-FISH	Catalyzed reporter deposition fluorescence in situ hybridization
DAPI	4',6-diamidino-2-phenylindole (fluorescent stain)
EUB 338	Most Bacteria Probe
DELTA 495	Deltaproteobacteria Probe
GEO A/B/C	Geobacter Cluster Probe
DIET	Direct interspecies electron transfer

## **Introduction**

**Literature Review.** Environmental microbiology has explored the role microorganisms in subsurface environments play in the iron cycle. Iron-reducing prokaryotes conserve energy for growth by transferring electrons from organic substrates to ferric iron (Fe(III)) oxides. These anaerobic microbes are widespread in sediments and soils due to the availability of ferric iron, which precipitates as ferric oxides at circumneutral pH. Microbes can perform the difficult process of extracellular electron transport by either physically contacting Fe(III) oxide particles, by excreting organic iron chelators to increase the solubility of Fe(III), or without physical contact using electron-shuttling compounds (Kappler et. al, 2005). Some iron-reducing bacteria can also pass electrons to other organisms by direct interspecies electron transfer (DIET) (Loveley et. al 2014).

Previous studies have shown that Deltaproteobacteria, specifically members of the Desulfuromonadales, are highly enriched in Fe(III)-reducing environments (Bray et al. 2017). Geobacteraceae, a family within the order Desulfuromonadales, is known for its ability to reduce Fe (III) and oxidize acetate through various mechanisms (Röling, 2014). Lake Matano Indonesia is a permanently stratified tropical lake boasting Iron rich anoxic sediments overlaid by an anoxic water column (Crowe et al. 2008). Therefore, Lake Matano is a novel yet understudied environment for characterizing iron reducing microorganisms.

**Description of research problem.** This study aimed to characterize the activity, morphology, and phylogeny of Fe(III)-reducing bacteria enriched from an anoxic, iron-rich (ferruginous) lake sediment from Lake Matano, Indonesia. We used a continuously stirred sequencing batch bioreactor (SBR) for anoxic enrichments in a freshwater enrichment medium to mimic environmental conditions. Fe(III) was provided in the form of amorphous Fe(III) oxide (ferrihydrite). We monitored Iron reduction and fixed bacterial samples for both DAPI and CARD-



FISH fluorescent microscopy analysis. Cell growth followed iron reduction rates meaning iron reducers were present in the sample exhibiting vibrio and bacillus morphologies. Instances of particle association and DIET interactions were found in microscopy samples providing an insight of possible electron transfer mechanisms. Furthermore, we found that 63% percent of cells were bacteria, 24% Deltaproteobacteria and 18% of cells pertained to the *Geobacter* cluster.

This physiological, morphologic, and phylogenetic characterization of Fe(III)-reducing bacteria is applicable to soil contaminant bioremediation and microbial fuel cells.

### **Methods and Materials**

In this study, a continuously stirred SBR was used for anoxic enrichments in a freshwater enrichment medium. Fe(III) was provided in the form of amorphous Fe(III) oxide (ferrihydrite). Iron reduction activity was measured by HCl-soluble Fe(II) concentration over time using ferrozine colorimetry. Catalyzed reporter deposition fluorescence in situ hybridization (CARD-FISH) was used to identify the phylogeny, morphology, and particle association of enriched bacteria. Probes targeting most *Bacteria* (EUB 338), *Deltaproteobacteria* (DELTA495A) and *Geobacter* (GEO3-A/B/C) were applied to cultured samples (Table 1).

### **Sample Collection and Storage**

A 15-cm sediment core from 200 m water depth in Lake Matano, Sulawesi Island, Indonesia (2°26'S, 121°15'E; in situ sediment temperature ~27°C), was sampled in November 2014 and subsampled at 5-cm increments (Bray et al., 2017). Sediments from 0–5 to 5–10 cm depth were fluffy and black, and 10–15 cm was dark gray. Sediments were sealed in gastight bags with no headspace (Hansen, Thamdrup, & Jørgensen, 2000) and stored at 4°C until incubation began in September 2017.

### **Enrichment Medium and Substrate Synthesis**

For mimicking environmental conditions, a freshwater enrichment medium lacking nitrate and sulfate developed based on the pore water composition of Lake Matano sediments (S.A. Crowe and D.A. Fowle, unpublished work) was used. The medium contained 825  $\mu\text{M}$   $\text{MgCl}_2$ , 550  $\mu\text{M}$   $\text{CaCO}_3$ , 3 mM  $\text{NaHCO}_3$ , 3.5  $\mu\text{M}$   $\text{K}_2\text{HPO}_4$ , 5  $\mu\text{M}$   $\text{Na}_2\text{HPO}_4$ , 225  $\mu\text{M}$   $\text{NH}_4\text{Cl}$ , 1  $\mu\text{M}$   $\text{CuCl}_2$ , 1.5  $\mu\text{M}$   $\text{Na}_2\text{MoO}_4$ , 2.5  $\mu\text{M}$   $\text{CoCl}_2$ , 23  $\mu\text{M}$   $\text{MnCl}_2$ , 4  $\mu\text{M}$   $\text{ZnCl}_2$ , 9.4  $\mu\text{M}$   $\text{FeCl}_3$  and 3 mM  $\text{Na}_2\text{NTA}$ , 0.07  $\mu\text{M}$  vitamin  $\text{B}_{12}$ , 0.4  $\mu\text{M}$  biotin, and 68.5  $\mu\text{M}$  thiamine.

Filter-sterilized vitamin and 500  $\mu\text{M}$  acetate solutions were added after autoclaving. Ferrihydrite ( $\text{Fe}(\text{OH})_3$ ) was synthesized as described in Schwertmann & Cornell (1991) and added to the bioreactor as described below in a periodic basis as described below.

### **Sediment Enrichment Culturing (Bioreactor Sediment enrichment)**

For enrichment culturing, Multifors 2 (INFORS HT) continuous stirred tank BSR of 500 mL volume was selected. To favor iron reduction, anaerobic conditions were maintained by constantly flushing the bioreactor with inert gas (90% $\text{N}_2$  and 10% $\text{CO}_2$  mix). To further prevent oxygen contamination, an Oxygen trap was placed between the gas tanks and the bioreactor gas inlets (Jeon, Dempsey Brian, Royer Richard, & Burgos William, 2004). Wasting was performed every 2 weeks, 250 mL BSR liquid content was replaced with new enrichment media and 500  $\mu\text{M}$  Ferrihydrite as substrate. For maintaining a circumneutral environment, pH and temperature were continuously monitored. The bioreactor culturing lasted 163 days.

### **HCl-extractable $\text{Fe}^{2+}$ and $\text{Fe}^{3+}$ and soluble $\text{Fe}^{2+}$**

Samples were taken from the bioreactor using a plastic syringe through the sampling port. The bioreactor sampling port was flushed with inert gas after sampling to prevent oxygen

contamination. To measure microbial activity HCl-extractable  $\text{Fe}^{2+}$  analyses were taken, 100  $\mu\text{l}$  of sediment slurry was extracted with 400  $\mu\text{l}$  0.6 N HCl in the dark for 30 minutes followed by measurement of 100  $\mu\text{L}$  supernatant and 900  $\mu\text{L}$  Ferrozine reagent in 46 mm HEPES (pH 8.3) mix at absorbance at 562 nm (Stookey, 1970) in spectrophotometer.

### **Microscopy: CARD-FISH with DAPI staining**

For the fixing process, 500  $\mu\text{L}$  of culture mix were fixed in 1 ml 4% PFA and incubated for 1 hour at room temperature. The samples were then tripled washed with 1ml of 0.2m filtered PBS after centrifuging for 5 min at 10,000 g. A volume of 500  $\mu\text{l}$  sample was filtered in a 0.45  $\mu\text{m}$  backing filter and 0.22  $\mu\text{m}$  polycarbonate filter using a vacuum at  $> 10$  mm Hg and washed with 1 ml of 0.2  $\mu\text{m}$  filtered PBS. The filters were then embedded with 0.2% low melting agarose, placed in a parafilm wrapped glass slide and dried at 45 C. Permeabilization followed by incubating the samples in Lysozyme (10 mg/mL) for 30-60 min, washed with  $\text{H}_2\text{O}$ , incubated in 0.01 M HCl for 15 min and tripled washed with  $\text{H}_2\text{O}$ . Hybridization was performed using 50 mL thin-walled falcon tubes as the humidity chamber skeleton, horseradish peroxidase (HRP) probe was added to the hybridization buffer to a concentration of 0.17 ng/ $\mu\text{L}$ , added to the filters and incubated for 3 hours at 46 C. After incubation, the filter was washed in pre-warmed washing buffer for 30 minutes at 48 C. Signal amplification was performed by dipping the filter in amplification buffer (1 : 1000 tyramide, .0015%  $\text{H}_2\text{O}_2$ ), placed onto parafilm covered slide, covered to keep at dark and incubated for 1 hr at 46 C. The following steps took place in dark conditions: washing with PBS and etOH and DAPI staining. Slides were stored at -20 C. Cell number per volume was obtained from cell counts using Image J.

Table 1 shows CARD-FISH probes.

**Table 1.** CARD-FISH probes utilized in this study

Common probe name	Generic name	Target(s)	Sequence (5'-3')	Position no.	Formamide Concentration	Reference
NON338	NA	None	ACTCCTACGGGA GGCAGC	NA	30 %	Wallner, Amann, and Beisker (1993)
EUB338-I	S-D-Bact-0338-a-A-18	Most <i>Bacteria</i>	GCTGCCTCCCGT AGGAGT	338-355	30 %	Amann et al. (1990)
DELTA495A	S-C-dProt-0495-a-A-18	Most <i>Delta proteobacteria</i>	AGTTAGCCGGTG CTTCCT	495-512	30 %	Loy et al. (2002)
GEO3-A	S-G-Geob-0818-a-A-21	<i>Geobacter</i> cluster	CCGCAACACCTA GTACTCATC	818-838	20% and 30%	Richter, Lanthier, Nevin, and Lovley (2007)
GEO3-B	S-G-Geob-0818-b-A-21		CCGCAACACCTA GTTCTCATC	818-838		
GEO3-C	S-G-Geob-0818-c-A-21		CCGCAACACCTG GTTCTCATC	818-838		

## **Results**

### **Iron Reduction**

Figure 1 shows Fe(II)-HCl ( $\mu\text{M}$ ) and number of cells (number /mL) in culture over the course of incubation. Iron reduction varied through the experiment with highest reduction period between days 80 and 100 of culture (**Figure 1**). Peak iron reduction was observed at day 98 with 997.1  $\mu\text{M}$  Fe (II)-HCl in culture. Medium-high reduction was observed at early stages (days 10-20) and later stages (days 120- 140) of culturing.

Cell number was consistent with iron reduction throughout the culturing period. Cell counts were from measurements taken at days 20, 42, 64, 86 and 126 from cell lighting with DAPI staining. Maximum cell counts were at sample days 64 and 86.

Iron reduction rates were consistent with cell counts, signifying iron reducers were enriched in the culture (**Figure 2**). The sample taken at day 64 showed the highest reduction rate per cell counts, meaning that cells sample at that day are the most representative or iron reducers.

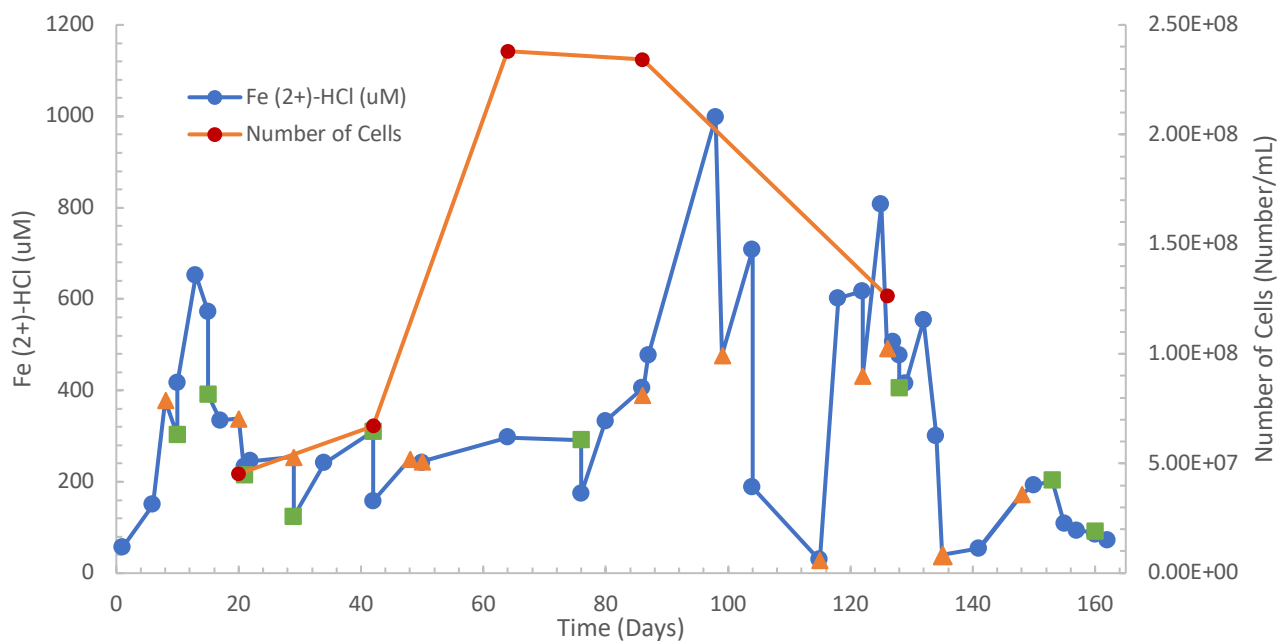


**Figure 1.** Fe(II)-HCl for the SBR bioreactor and cell number in time. Total culturing time of 163 days. Green squares represent 250 mL wasting and orange triangles represent 500 µL Ferrihydrite added.

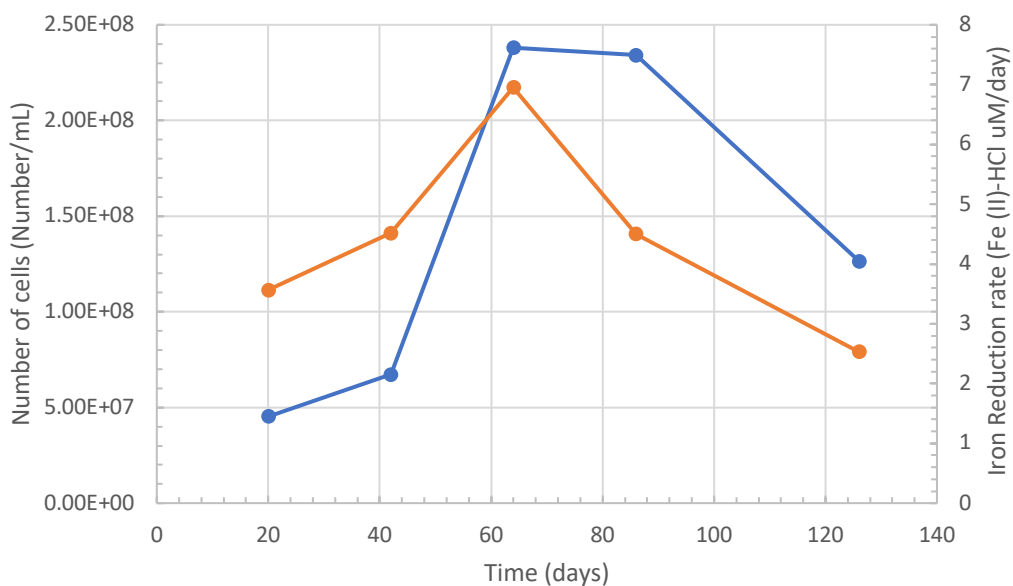


**Figure 2.** Iron reduction rates in orange and cell count in blue for the SBR bioreactor through time.

## Morphology

We observed various cell morphologies at days 20, 42, 64, 86 and 126 of culture incubation including coccus, filamentous, bacillus and vibrio (**Figure 3**). By 64, only bacillus and vibrio morphologies were observed. At day 64, samples were taken from the top and bottom of the vessel after a non-stirring period of 2 weeks. Top samples were abundant in bacillus morphology (75%) while bottom samples were abundant in vibrio morphology (96%).

We noticed that many of the cells from our culture formed aggregates (see supplemental material). Highest number of cells in aggregates were observed in day 64 from top samples (65%). Bottom samples show the least number of cells in aggregate (3%) (**Figure 4**). All cells in aggregates expressed a bacillus morphology. Percent cells in aggregate decreased with time (**Figure 5**).

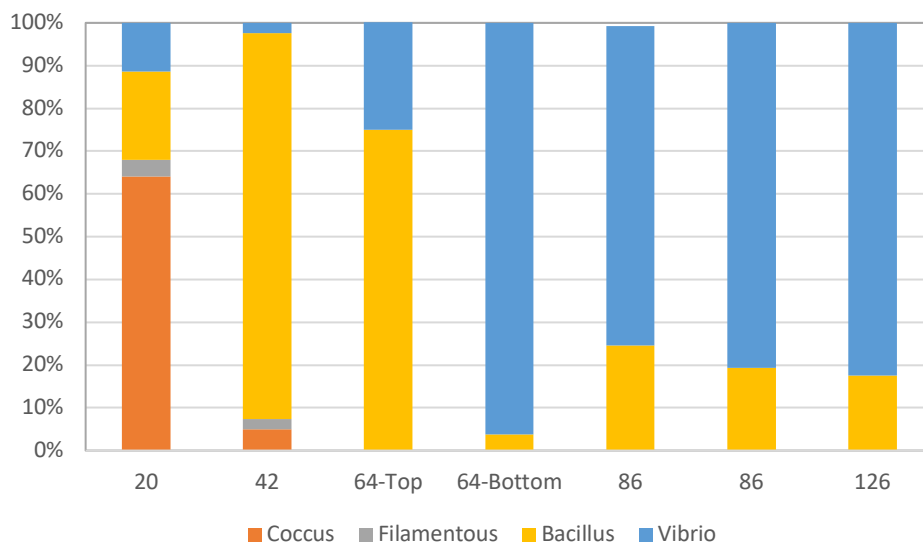


**Figure 3.** Observed culture morphologies from DAPI stained images at 100x.

We then used CARD-FISH to identify specific bacterial taxa from our cultures under the microscope at days 86 (EUB and DELTA probes) and 126 (GEO-A/B/C probe). Fluorescing morphologies included bacillus and vibrio. Most eubacteria showed a vibrio (61%) morphology

while delta proteobacteria probe fluorescing cells were mainly bacillus (79%). All *Geobacter* probe fluorescing cells were bacillus.

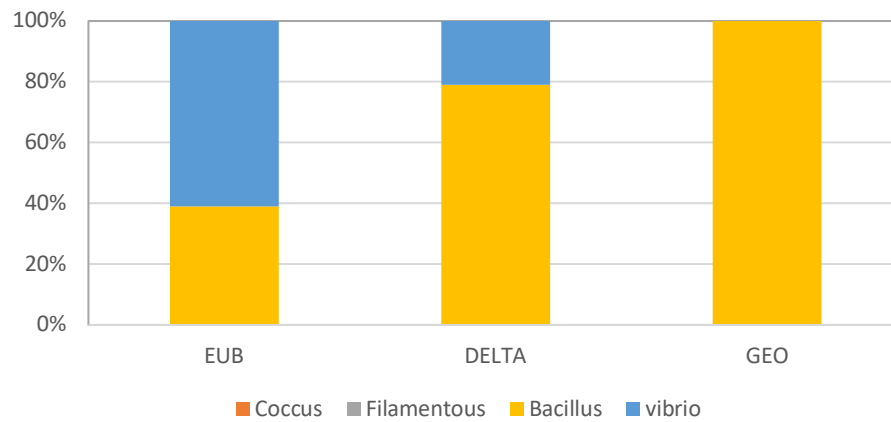


**Figure 4.** Observed culture morphologies from fluorescing cells from CARD-FISH microscopy at 100x augmentation.

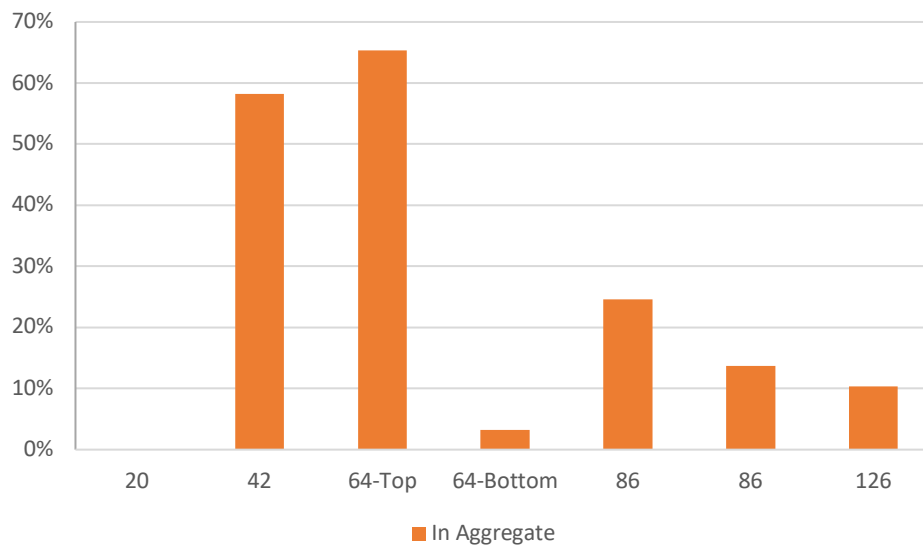


**Figure 5.** Percent cells in aggregate from DAPI stained images at 100x.

All cells in aggregate expressed a bacillus morphology. At day 86, fluorescing cells of EUB and DELTA probes showed aggregates formation (39% and 29% of cells respectively). At day 126, fluorescing cells of GEO-A/B/C probe showed a lower number of cells in aggregates (15%). Not all cells in aggregate at day 126 fluoresced with the GEO-A/B/C probes.



**Figure 6.** Percent cells fluorescing in aggregate from CARD-FISH microscopy at 100x augmentation.

## Phylogeny

As expected most cultured microorganisms were bacteria EUB 338 (63%), from the total cell counts a quarter were deltaproteobacteria DELTA 495A (24%) or 38% of bacteria were deltaproteobacteria and from total cell counts about a fifth were from the geobacter genus GEO-A/B/C (18%) or 75% of all deltaproteobacteria were from the geobacter cluster (**figure 7**).



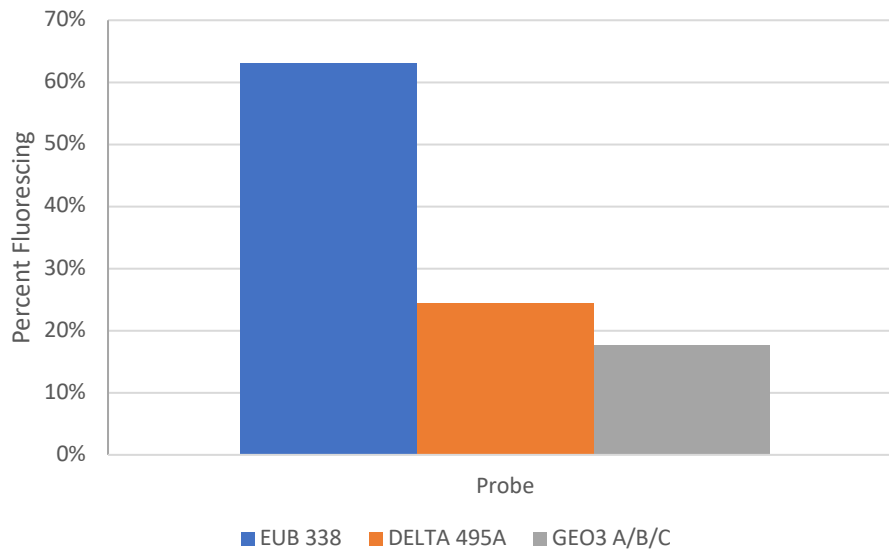


**Figure 7.** Relative abundance from CARD-FISH microscopy.

## **Discussion**

### **Iron reduction**

Cell counts correlated with iron reduction throughout the culturing period indicating iron reducing microorganisms were present in the environmental sample. Iron reducing microorganisms have been determined in other environmental sediments studies (Potomac River (Lovley & Phillips, 1988) and Coonamessett River (Erbs & Spain, 2002)). As expected, iron reduction increased with time given that the system favored culturing of iron reducing microorganisms.

### **Morphology**

Filamentous, coccus, bacillus and vibrio morphologies were observed through the culturing period with vibrio and bacillus being predominant at later stages of the culture. As observed in the results from DAPI staining images and CARD-FISH images through the evolution of the experiment, aggregates in the samples were consistent. Aggregates consisted of mainly bacillus morphologies,

vibrio was also identified in aggregate formations at later stages of the culture in DIET formations. At lower iron reduction rates (early stages of culture), filamentous and coccus morphologies were identified meaning that other microorganisms present in the lake sediment do not favor iron reduction.

## **Phylogeny**

As expected, bacteria were identified as the dominant domain in the lake sediment microbiome. Only a quarter of total cells were deltaproteobacteria and a fifth of total cells were from the geobacter genus. Given that iron reduction rates were significant at the time of CARD-FISH sampling it is possible that other iron reducing clusters (not Geobacter) were capable of contributing to the iron reduction rates.

## **Particle Association**

Particle association instances were observed at days 20, 62, 86 and 126 (see supplemental material) from single cell associations to ferrihydrite particles. Particle association was observed using the GEO3 A/B/C probe at day 126 in rod like cells (from probe fluorescence it is hard to determine the morphology, either vibrio or bacillus, of the attached cells).

## **DIET**

As seen in day 86 samples, DIET interactions occurred in members from bacteria (green lighting probe) and other non-bacteria microorganisms (archaea). It can be observed that another DIET interaction was observed with the DELTA 495 probe but it is unclear if the non-fluorescing microorganisms pertain to the bacteria domain.

### **Future work**

In the future, DNA extraction and polymerase chain reaction (PCR) amplification of the 16S rRNA gene could be used to determine the dominant species. Genomic characterization for the fixed samples, look at cytochrome proteins in genomic databases and SEM images for nanowires identification in particle association instances.

### **Acknowledgements**

The author thanks Marcus S. Bray for technical assistance and the Louis Stokes Alliance for Minority Participation (LSAMP) from the National Science Foundation for its financial support.

## **References**

- Amann, R. I., Ludwig, W., & Schleifer, K. H. (1995). Phylogenetic identification and in situ detection of individual microbial cells without cultivation. *Microbiological Reviews*, 59(1), 143–169.
- Amann, R. I., B. J. Binder, R. J. Olson, S. W. Chisholm, R. Devereux, and D. A. Stahl. (1990). Combination of 16S rRNA-targeted oligonucleotide probes with flow cytometry for analyzing mixed microbial populations. *Appl. Environ. Microbiol.* 56:1919-1925
- B. A. Methé, K. E. N., J. A. Eisen, I. T. Paulsen, W. Nelson, J. F. Heidelberg, D. Wu, M. Wu, N. Ward, M. J. Beanan, R. J. Dodson, R. Madupu, L. M. Brinkac, S. C. Daugherty, R. T. D., A. S. Durkin, M. Gwinn, J. F. Kolonay, S. A. S., D. H. Haft, J. Selengut, & T. M. Davidsen, N. Z., O. White, B. Tran, C. Romero, H. A. Forberger, J. Weidman, H. Khouri, T. V. Feldblyum, T. R. Utterback, S. E. Van Aken, D. R. Lovley, C. M. Fraser. (2003). Genome of *Geobacter sulfurreducens*: Metal Reduction in Subsurface Environments. *Science*.
- Bray, M. S., Wu, J., Reed, B. C., Kretz, C. B., Belli, K. M., Simister, R. L., . . . Glass, J. B. (2017). Shifting microbial communities sustain multiyear iron reduction and methanogenesis in ferruginous sediment incubations. *Geobiology*, 15(5), 678-689. doi:10.1111/gbi.12239
- Crowe, S. A., O'Neill, A. H., Katsev, S., Hehanussa, P., Haffner, G. D., Sundby, B., . . . Fowle, D. A. (2008). The biogeochemistry of tropical lakes: A case study from Lake Matano, Indonesia. *American Society of Limnology and Oceanography, Inc.*, 53(1), 319-331.
- Erbs, M., & Spain, J. (2002). Microbial iron metabolism in natural environments. *Microbial Diversity*, 2002.
- Holmes, D. E., Nicoll, J. S., Bond, D. R., & Lovley, D. R. (2004). Potential role of a novel psychrotolerant member of the family Geobacteraceae, *Geopsychrobacter electrodiphilus* gen. nov., sp. nov., in electricity production by a marine sediment fuel cell. *Appl Environ Microbiol*, 70(10), 6023-6030.
- Jeon, B.-H., Dempsey Brian, A., Royer Richard, A., & Burgos William, D. (2004). Low-Temperature Oxygen Trap for Maintaining Strict Anoxic Conditions. *Journal of Environmental Engineering*, 130(11), 1407-1410. doi:10.1061/(ASCE)0733-9372(2004)130:11(1407)
- Kappler, A. (2005). Geomicrobiological Cycling of Iron. *Reviews in Mineralogy and Geochemistry*, 59(1), 85-108. doi:10.2138/rmg.2005.59.5
- Lovley, D. R., & Phillips, E. J. P. (1988). Novel Mode of Microbial Energy Metabolism: Organic Carbon Oxidation Coupled to Dissimilatory Reduction of Iron or Manganese. *Appl Environ Microbiol*, 54(6), 1472-1480.
- Lovley, D. R., & Phillips, E. J. P. (1988). Novel Mode of Microbial Energy Metabolism: Organic Carbon Oxidation Coupled to Dissimilatory Reduction of Iron or Manganese. *Applied and Environmental Microbiology*, 54(6), 1472.

Loy, A., A. Lehner, N. Lee, J. Adamczyk, H. Meier, J. Ernst, K. H. Schleifer, and M. Wagner. 2002. Oligonucleotide microarray for 16S rRNA gene-based detection of all recognized lineages of sulfate-reducing prokaryotes in the environment. *Appl. Environ. Microbiol.* 68:5064-5081.

Malvankar, N. S., & Lovley, D. R. (2014). Microbial nanowires for bioenergy applications. *Curr Opin Biotechnol*, 27, 88-95.

Mahadevan, R., Bond, D. R., Butler, J. E., Esteve-Nunez, A., Coppi, M. V., Palsson, B. O., . . . Lovley, D. R. (2006). Characterization of metabolism in the Fe(III)-reducing organism *Geobacter sulfurreducens* by constraint-based modeling. *Appl Environ Microbiol*, 72(2), 1558-1568.

Röling, W. F. M. (2014). The Family Geobacteraceae The Prokaryotes. 157-172.

Richter, H., Lanthier, M., Nevin, K. P., & Lovley, D. R. (2007). Lack of Electricity Production by *Pelobacter carbinolicus* Indicates that the Capacity for Fe(III) Oxide Reduction Does Not Necessarily Confer Electron Transfer Ability to Fuel Cell Anodes . *Applied and Environmental Microbiology*, 73(16), 5347–5353.

Shi, L., Dong, H., Reguera, G., Beyenal, H., Lu, A., Liu, J., . . . Fredrickson, J. K. (2016). Extracellular electron transfer mechanisms between microorganisms and minerals. *Nat Rev Microbiol*, 14(10), 651-662.

Shun'ichi Ishii & Bruce E. Logan & Yuji Sekiguchi (2012). Enhanced electrode-reducing rate during the enrichment process in an air-cathode microbial fuel cell. *Appl Microbiol Biotechnol*. 94:1087–1094

Wallner, G., R. Amann, and W. Beisker. 1993. Optimizing fluorescent in situ hybridization with rRNA-targeted oligonucleotide probes for flow cytometric identification of microorganisms. *Cytometry* 14:136-143.

## SUPPLEMENTAL MATERIAL

Figures 1, 2, 3 and 4 at days 20, 42, 62 (top) and 62 (bottom) respectively, show the microscopy observations at 100x augmentation with DAPI staining.

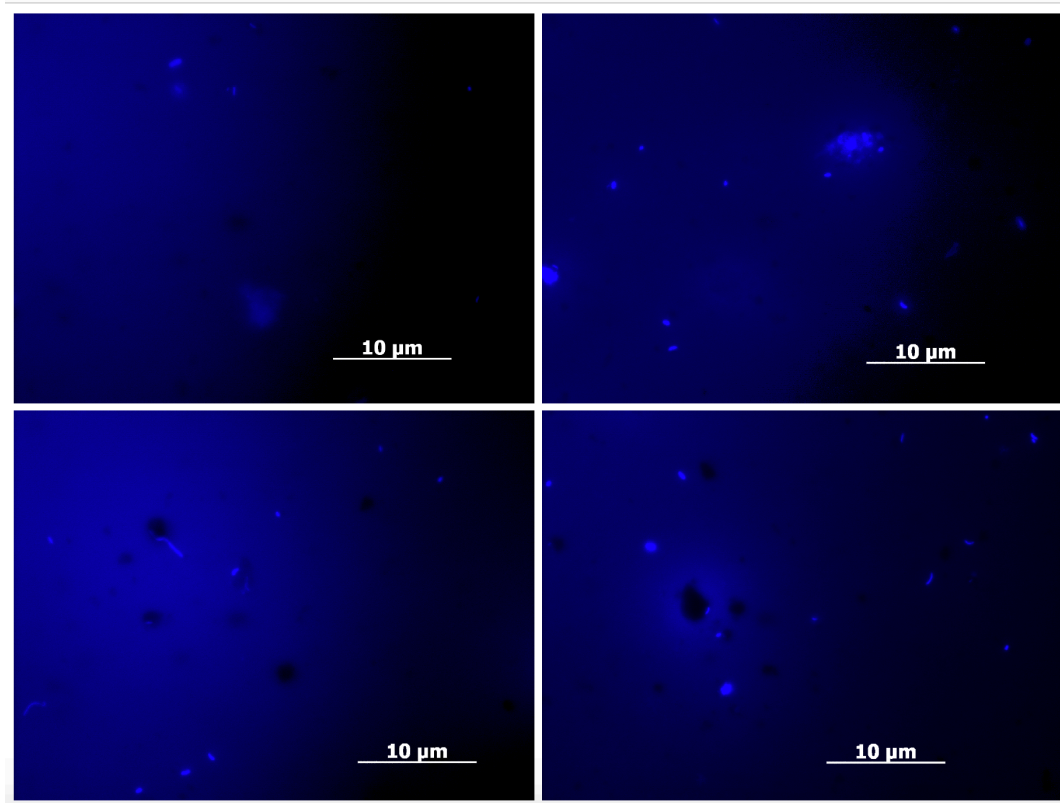


**Figure 1.** Microscopy with DAPI staining at day 20

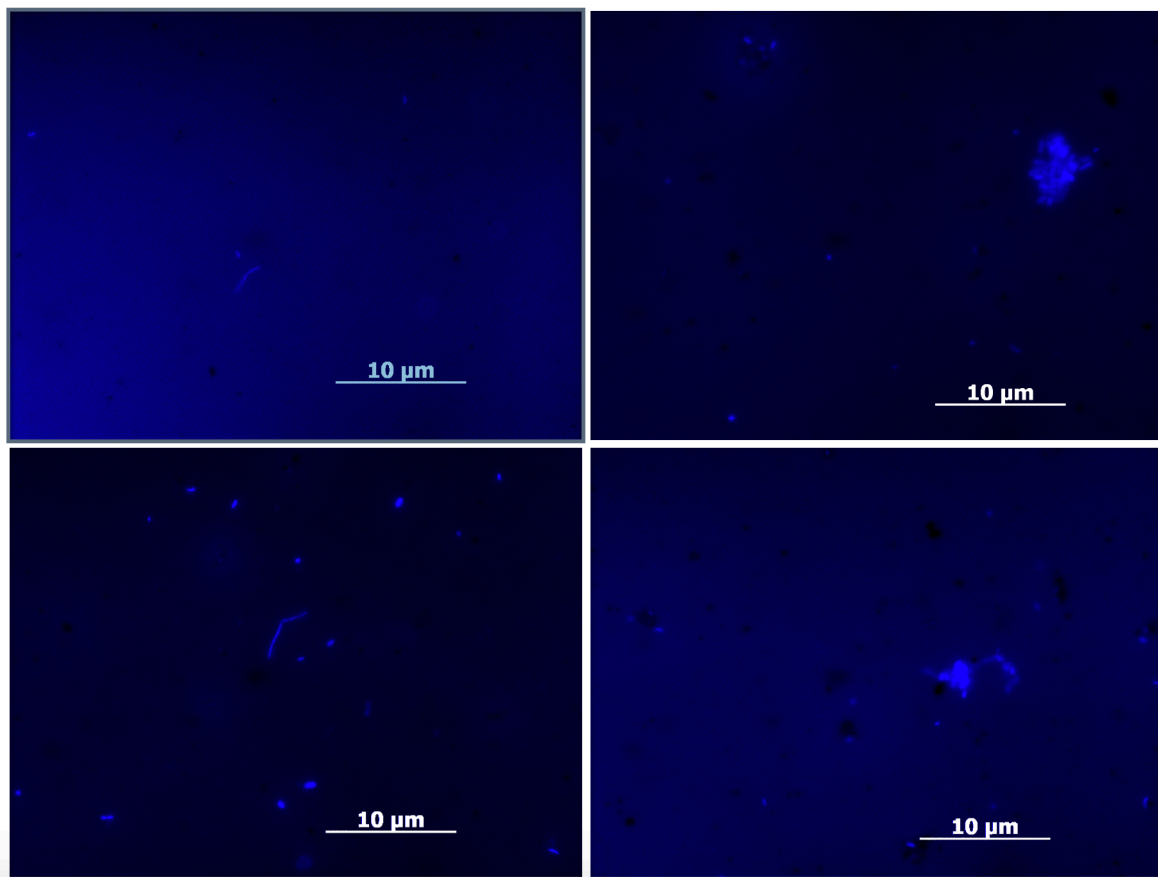


**Figure 2.** Microscopy with DAPI staining at day 42.

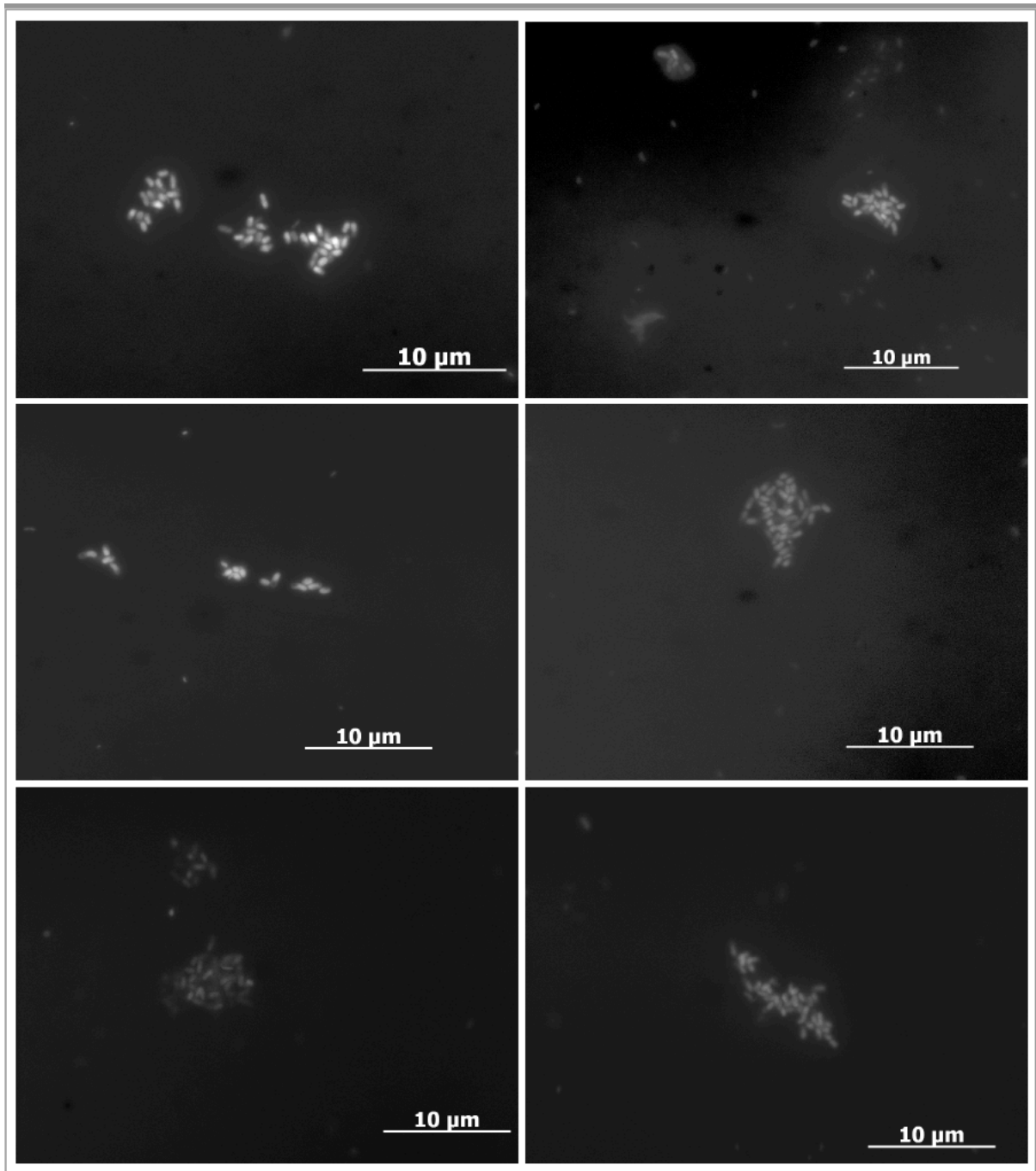


**Figure 3.** Microscopy with DAPI staining at day 62, top of reactor.



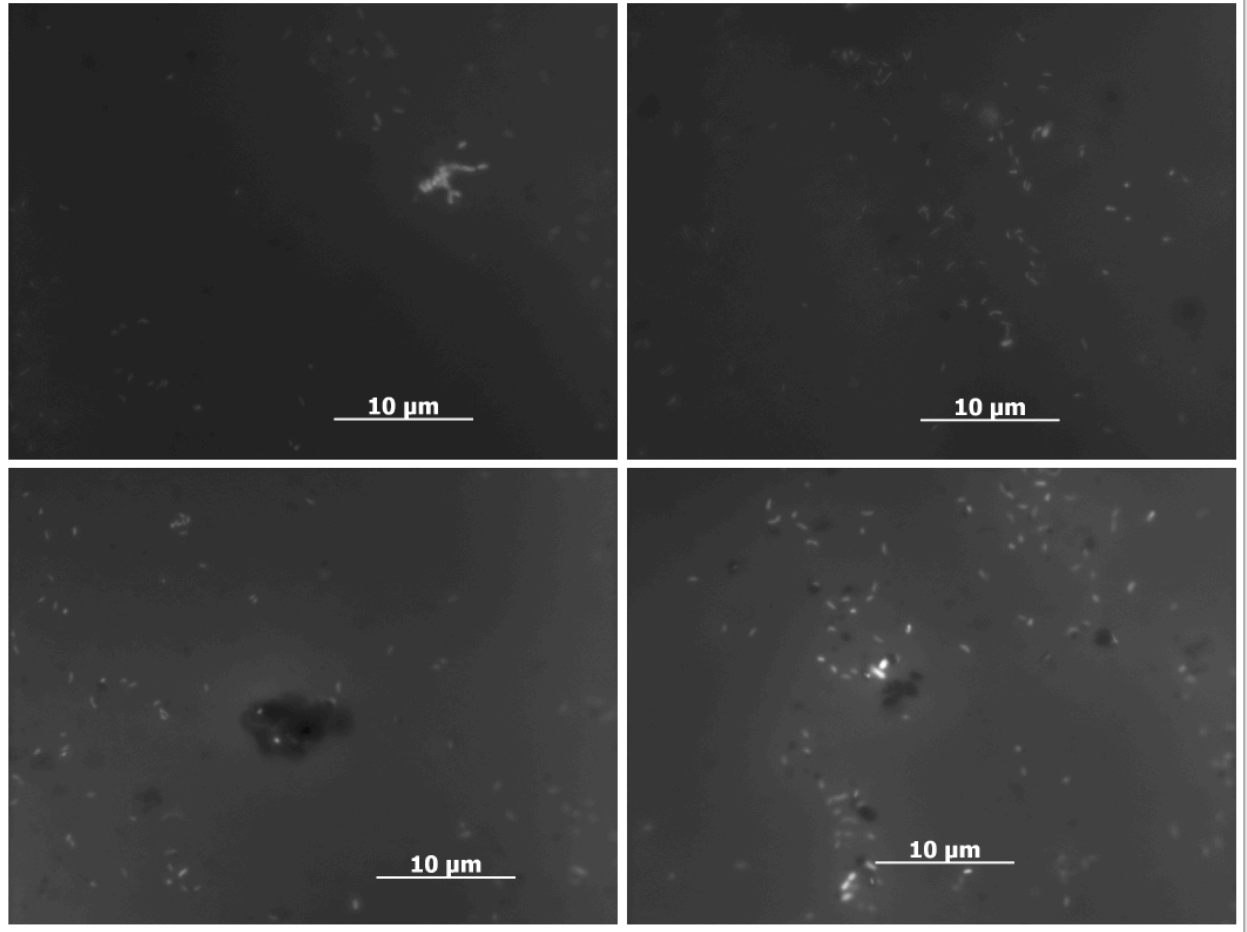


**Figure 4.** Microscopy with DAPI staining at day 62, bottom of reactor.

Figures 5, 6 and 7 show the microscopy observations from the EUB 338, DELTA 495A and GEO-A/B/C probes under 100x augmentation under GFP light.

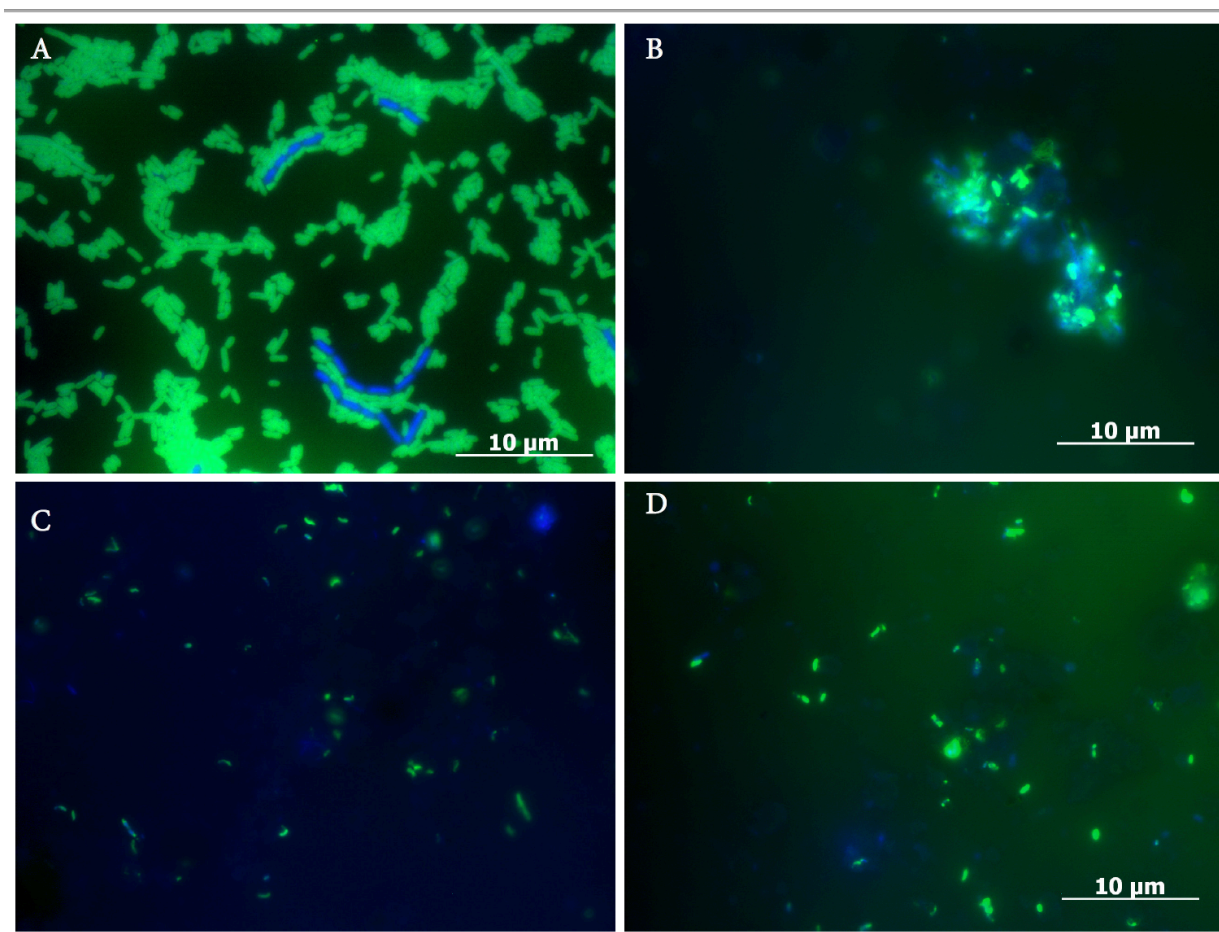


**Figure 5.** EUB 338 probe, DAPI staining (blue) and probe fluorescing (green). A. Control *e. coli*. B. Aggregate. C. Scattered cells. D. Scattered cells

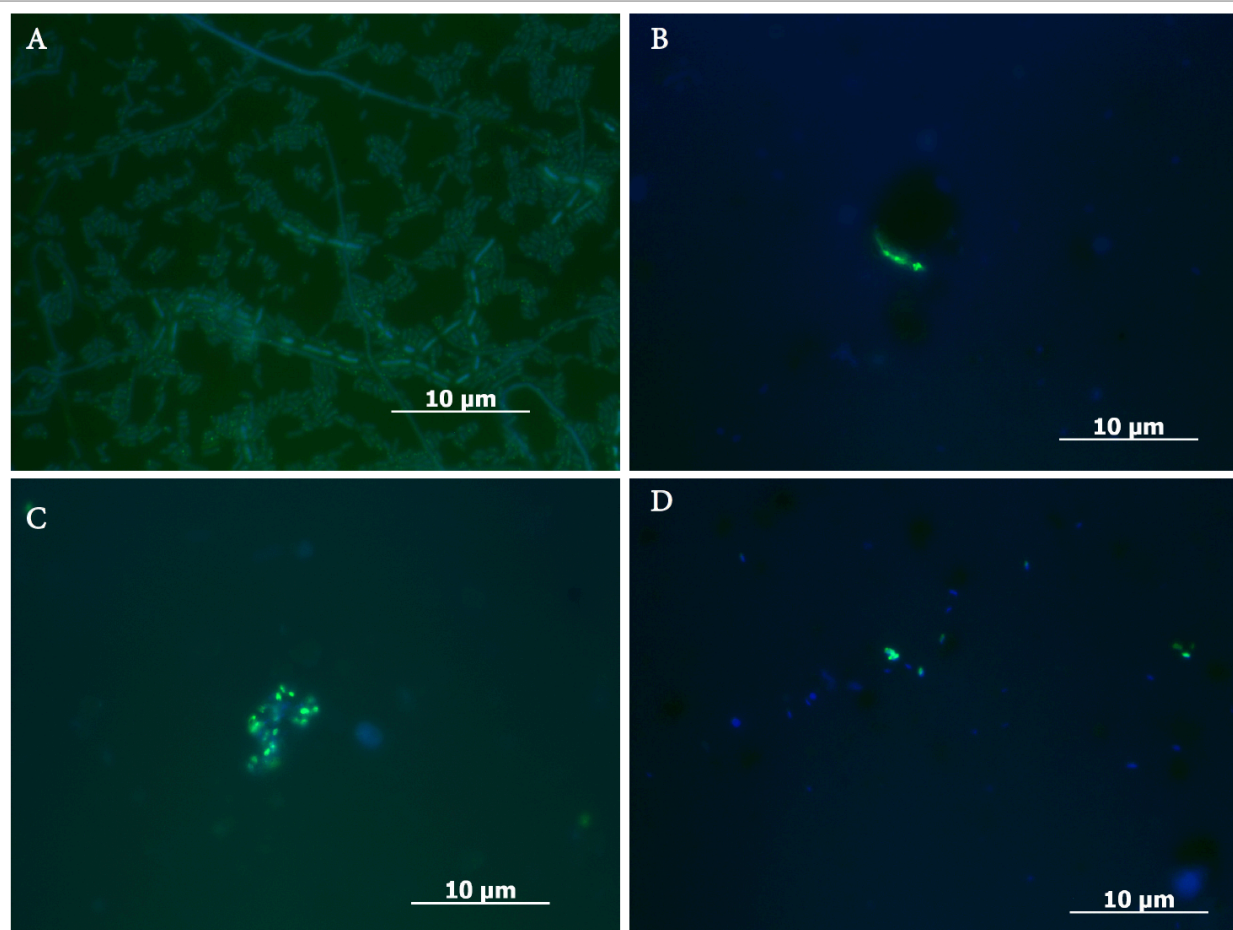


**Figure 6.** DEL 495A probe, DAPI staining (blue) and probe fluorescing (green). A. Control *e. coli*. B. Particle association. C Aggregate. D. Scattered cells.

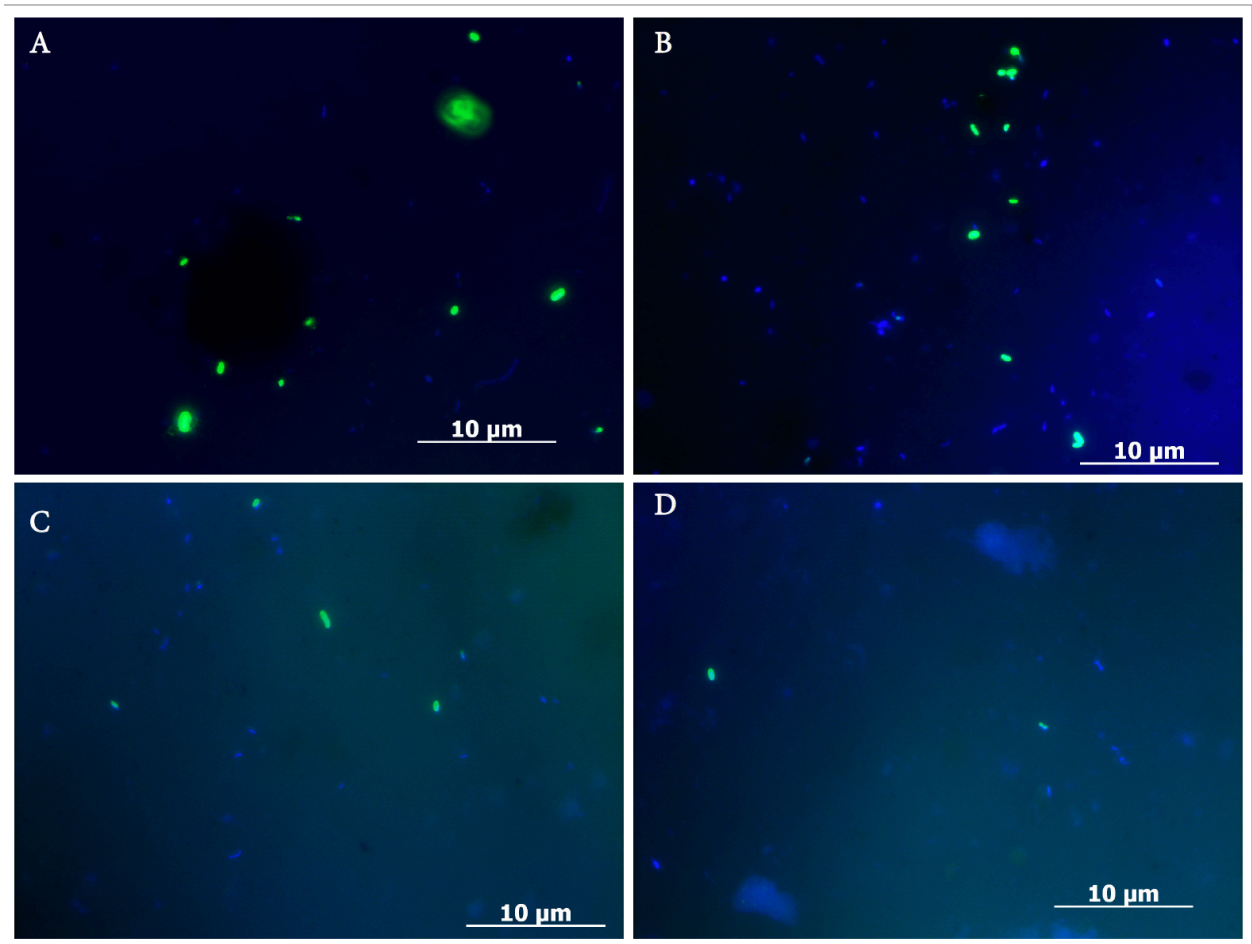


**Figure 7.** GEO- A/B/C probe, DAPI staining (blue) and probe fluorescing (green). A. Particle association. B. Scattered cells. C Scattered cells. D. Scattered cells.